Living specimen tomography by digital holographic microscopy: morphometry of testate amoeba

Florian Charrière, Nicolas Pavillon, Tristan Colomb and Christian Depeursinge

Ecole Polytechnique Fédérale de Lausanne (EPFL), Imaging and Applied Optics Institute, CH-1015 Lausanne, Switzerland
florian.charriere@a3.epfl.ch

http://apl.epfl.ch/page12232.html

Thierry J. Heger[a,b] and Edward A.D. Mitchell[a,b]

[a]*Swiss Federal Research Institute WSL, CH-1015 Lausanne, Switzerland.*
[b]*Ecole Polytechnique Fédérale de Lausanne (EPFL), Laboratory of Ecological Systems, CH-1015 Lausanne, Switzerland.*

http://ecos.epfl.ch/

Pierre Marquet

Centre de Neurosciences Psychiatriques, Département de psychiatrie DP-CHUV, Site de Cery, CH-1008 Prilly-Lausanne, Switzerland

Benjamin Rappaz

Ecole Polytechnique Fédérale de Lausanne (EPFL), Brain Mind Institute, CH-1015 Lausanne, Switzerland

Abstract: This paper presents an optical diffraction tomography technique based on digital holographic microscopy. Quantitative 2-dimensional phase images are acquired for regularly-spaced angular positions of the specimen covering a total angle of π, allowing to built 3-dimensional quantitative refractive index distributions by an inverse Radon transform. A 20x magnification allows a resolution better than 3 μm in all three dimensions, with accuracy better than 0.01 for the refractive index measurements. This technique is for the first time to our knowledge applied to living specimen (testate amoeba, Protista). Morphometric measurements are extracted from the tomographic reconstructions, showing that the commonly used method for testate amoeba biovolume evaluation leads to systematic under evaluations by about 50%.

OCIS codes: (090.1760) Computer holography; (110.6880) Three-dimensional image acquisition; (110.6960) Tomography; (170.6900) Three-dimensional microscopy.

References and links

1. A. Dunn, Light scattering properties of cells, PhD Diss., Univ. of Texas, Austin, 1997.
2. J. Bereiter-Hahn, Cecil H. Fox and BO Thorell, "Quantitative reflection contrast microscopy of living cells," J. Cell Biol. **82**, 767-779 (1979).
3. C. L. Curl, C. J. Bellair, T. Harris, B. E. Allman, P. J. Harris, A. G. Stewart, A. Roberts, K. A. Nugent and L. M. D. Delbridge, "Refractive index measurement in viable cells using quantitative phase-amplitude microscopy and confocal microscopy," Cyt. A **65**, 88 (2005).
4. B. Rappaz, P. Marquet, E. Cuche, Y. Emery, C. Depeursinge, and P. Magistretti, "Measurement of the integral refractive index and dynamic cell morphometry of living cells with digital holographic microscopy," Opt. Express **13**, 9361-9373 (2005).

#71852 - $15.00 USD Received 9 June 2006; revised 20 July 2006; accepted 24 July 2006

5. E. Wolf, "Three-dimensional structure determination of semi-transparent object from holographic data," Opt. Commun. **1**, 153–156 (1969).
6. R. Dändliker, K. Weiss, "Reconstruction of three-dimensional refractive index from scattered waves," Opt. Commun. **1**, 323–328 (1970).
7. V. Lauer, "New approach to optical diffraction tomography yielding a vector equation of diffraction tomography and a novel tomographic microscope," J. Microsc. **205**, 165–176 (2002).
8. G. N. Vishnyakov, G. G. Levin, "Optical microtomography of phase objects, " Opt. Spectrosc. **85**, 73-77 (1998).
9. G. N. Vishnyakov, G. G. Levin, A. V. Likhachev, V. V. Pikalov, "Phase Tomography of 3D Biological Microobjects: Numerical Simulation and Experimental Results," Opt. Spectrosc. **87**, 413-419 (1999).
10. A. Barty, K.A. Nugent, A. Roberts, D. Paganin, "Quantitative phase tomography," Opt. Commun. **175**, 329-336 (2000).
11. T. Noda, S. Kawata and S. Minami, "Three-dimensional phase-contrast imaging by a computed-tomography microscope", Appl. Opt. **31**, 670-674 (1992).
12. F. Charrière, F. Montfort, J. Kühn, T. Colomb, A. Marian, E. Cuche, P. Marquet, and Ch. Depeursinge, "Cell refractive index tomography by digital holographic microscopy," Opt. Lett. **31**, 178-180 (2006).
13. E. A. D. Mitchell, A. Buttler, B. Warner and J.-M. Gobat, "Ecology of testate amoebae (Protozoa: Rhizopoda) in *Sphagnum*-dominated peatlands in the Jura Mountains, Switzerland and France," Ecoscience **6**, 565-576 (1999).
14. E. A. D. Mitchell, D. J. Charman and B. G. Warner, "Testate amoebae analysis in ecological and paleoecological studies of wetlands: past, present and future," Biodivers. Conserv. (to be published).
15. H. Nguyen-Viet, N. Bernard, E. A. D. Mitchell, J. Cortet, P. M. Badot and D. Gilbert, "Relationship between testate amoebae and atmospheric heavy metals (Pb, Cd, Zn, Ni, Cu, Mn and Fe) accumulated in the moss *Barbula indica* Hanoi, Vietnam," Microbial Ecol. (to be published).
16. R. E. Madrid and C. J. Felice, "Microbial biomass estimation," Crit. Rev. Biotechnol., **25**, 97-112 (2005).
17. D. Gilbert, C. Amblard, G. Bourdier and A.-J. Francez, "The microbial loop at the surface of a peatland: Structure, function, and impact of nutrient input," Microbial Ecol. **35**, 83-93 (1998).
18. E. A. D. Mitchell, D. Gilbert, A. Buttler, P. Grosvernier, C. Amblard and J.-M. Gobat, "Structure of microbial communities in *Sphagnum* peatlands and effect of atmospheric carbon dioxide enrichment," Microbial Ecol. **16**, 187-199 (2003).
19. E. Cuche, P. Marquet, and C. Depeursinge, "Simultaneous amplitude-contrast and quantitative phase-contrast microscopy by numerical reconstruction of Fresnel off-axis holograms," Appl. Opt. **38**, 6994-7001 (1999).
20. T. Colomb, E. Cuche, F. Charrière, J. Kühn, N. Aspert, F. Montfort, P. Marquet, and Ch. Depeursinge, "Automatic procedure for aberration compensation in digital holographic microscopy and applications to specimen shape compensation," Appl. Opt. **45**, 851-863 (2006).
21. F. Charrière, E. Cuche, P. Marquet, C. Depeursinge, "Biological cell (pollen grain) refractive index tomography with digital holographic microscopy." in *Three-Dimensional and Multidimensional Microscopy: Image Acquisition and Processing XIII*, J.-A. Conchello, C.J. Cogswell, T. Wilson, eds., Proc. SPIE **6090**, 22-29 (2006).
22. P. Marquet, B. Rappaz, P. J. Magistretti, E. Cuche, Y. Emery, T. Colomb and C. Depeursinge, "Digital holographic microscopy: a noninvasive contrast imaging technique allowing quantitative visualization of living cells with subwavelength axial accuracy," Opt. Lett. **30**, 468-470 (2005).
23. P. Marquet, "Développement d'une nouvelle technique de microscopie optique tridimensionnelle, la microscopie holographique digitale. Perspective pour l'étude le la plasticité neuronale," MD-PhD Thesis Dissertation (Chapt. 5), UNI-Lausanne, 2003.
24. A. C. Kak and M. Slaney. Principles of Computerized Tomographic Imaging. Soc. of Ind. and Appl. Math. SIAM, 2001.
25. T. C. Wedberg, J. J. Stamnes and W. Singer, "Experimental examination of the quantitative imaging properties of optical diffraction tomography," J. Opt. Soc. Am. A **12**, 493-500 (1995).
26. W. Singer, T. C. Wedberg, and J. J. Stamnes, "Comparison of the filtered backpropagation and the filtered backprojection algorithms for quantitative tomography," Appl. Opt. **34**, 6575-6581 (1995).
27. E. A. Paul and F. E. Clark, Soil microbiology and biochemistry, (Second Edition, Academic Press, San Diego, CA. 1996).
28. M. Bölter, J. Bloem, K. Meiners and R. Möller, "Enumeration and biovolume determination of microbial cells - a methodological review and recommendations for applications in ecological research," Biol. Fert. Soils **36**, 249-259 (2002).
29. Dr. Enrique Lara, Swiss Federal Research Institute WSL and Laboratory of Ecological Systems, Ecole Polytechnique Fédérale de Lausanne (EPFL), CH-1015 Lausanne, Switzerland. (personnal communication, 2006).

#71852 - $15.00 USD Received 9 June 2006; revised 20 July 2006; accepted 24 July 2006

1. Introduction

Optical microscopy techniques nowadays offer non-contact, high-resolution and real-time cell imaging facilities. Though, the knowledge of the optical properties of the intracellular organelles is deemed to bring valuable information about cells morphology, cellular internal processes or organelles spatial distribution. A good review of the available techniques and refractive indices in the literature can be found in Ref. 1. Besides the techniques quoted in Ref. 1, different approaches developed to measure the refractive index (RI) of cells should be mentioned. Bereiter-Hahn *et al.* have studied the refractive index variation at the surface of mammalian cells in culture with quantitative reflection contrast microscopy.[2] More recently, Curl *et al.* have compared height measurement achieved with a confocal microscope and optical path length (OPL) measurements with a phase-sensitive technique to deduce the integrated RI through a muscle cell.[3] *Rappaz et al.* have followed dynamically the integrated RI through neuronal cells during a hypotonic stress, comparing absolute phase measurements obtained with digital holographic microscopy for two different perfusion solutions.[4] However, these last two approaches allow to measure the 2D planar distribution of the RI integrated along the optical axis, making the visualization of individual intracellular organelles difficult.

A well-suited technique to address this particular problematic of measuring the 3-dimentionnal (3D) refractive index distribution of a cell, is the so-called optical diffraction tomography (ODT), which theoretical bases have been developed by Wolf[5] and Dändliker[6] in the early seventies. ODT allows, by recording the complex wavefront diffracted by a transparent or semi-transparent object under varying illumination angles, to reconstruct its 3D scattering potential. Lauer used for example phase-shifting interferometry (PSI) to record the Fourier spectrum of the diffracted wavefront, varying the illumination direction by changing the direction of the beam itself.[7] Vishnyakov and Levin combined PSI with a Linnik interferometer also allowing multiple angles illumination.[8-9] Barty *et al.* developed a phase-retrieval algorithm, based on 3 intensity measurements performed on different focus planes, combined with a rotation of the specimen relatively to a fixed illumination beam.[8] There are really few successful applications of ODT techniques to living specimen imaging, mainly due to the difficulty of measuring accurately the complex diffracted wavefront: Lauer used his tomographic microscope to observe bacteria and yeasts,[7] Noda *et al.* investigated green mold (*Aspergillus oryzae*),[9] and Vishnyakov and Levin observed human red blood cells and lymphocites.[8-9] Note that quantitative RI data are found only in Refs. 8-9.

In a recent paper,[12] we have shown for the first time to our knowledge the quantitative 3D distribution of RI of a semi-transparent object, in our case a pollen grain, provided by backprojecting OPL values collected with digital holographic microscopy (DHM) on a series of projections of the preparation taken at various incidence angles. The accuracy of the RI determination was better than 0.01, and the 3D spatial resolution better than 1 μm in all 3D. Furthermore, DHM reconstructs the complex diffracted wavefront from a single hologram for each orientation of the specimen, while at least 3 images are required for PSI, reducing this way the acquisition time and the stability requirements for the system.

In the present paper, the system described in Ref. 12 has been further developed, to allow the first investigation of living biological specimens, thanks to a specifically designed observation chamber. The reconstructed 3D RI distributions, revealing intracellular structures, have permitted to accurately measure the volume of the specimen. The biological specimen observed, presented in Fig. 1, is a testate (or shelled) amoeba ("protozoa", more specifically a protist belonging to the Amoebozoa), *Hyalosphenia papilio*, with a shell approximately 130 μm long, 70 μm wide and 35 μm deep.

This species is commonly found in nutrient-poor peatlands, and the specimens presented in this work were collected in moss (*Sphagnum*) from Praz-Rodet Bog, Canton Vaud, Switzerland (46°33' N, 06°10' E). It is one of the few protozoa to house endosymbiotic algae, visible as small green spheres in Fig. 1(a), and hence its metabolism is referred to as mixotrophy, i.e. combing auto- and heterotrophy). Because of this interesting metabolism, its commonness in peatlands, and its characteristic morphology making it easily identifiable, it

#71852 - $15.00 USD Received 9 June 2006; revised 20 July 2006; accepted 24 July 2006

may represent a good candidate as a model organism for studies in population ecology or ecotoxicology.[13] Beyond the interest for a specific species, testate amoebae are increasingly used in community ecology with applications in the reconstruction of past climates (paleoecology),[14] the monitoring of pollution[15] or environmental changes. In many of these applications it is important to have precise estimates of cell volume. This allows the calculation of the biomass with the help of an appropriate conversion factor.[16] The biovolume is usually achieved using simple measurements and assuming geometrical shapes, but it is unclear if these correspond very well to the reality.[17-18] A much better approach would be to quantify exactly the volume and to determine how this compares to some easily measurable variable such as the length or width. If a clear correlation can be established in such as way for a number of specimens of each species, or morphological type for closely-related species, this data can then be used to derive allometric relationships that can be used in a standard way forever. Another interesting aspect is the presence of endosymbiotic algae. These may also respond to changes in the environment indirectly through the amoeba itself or directly if some contaminant enters the amoeba cell without affecting it directly. It would therefore be interesting to be able to quantify the number of algal cells and their individual volumes. This is clearly not possible using light microscopy, as in Fig. 1(a), but may be possible using holographic tomography.

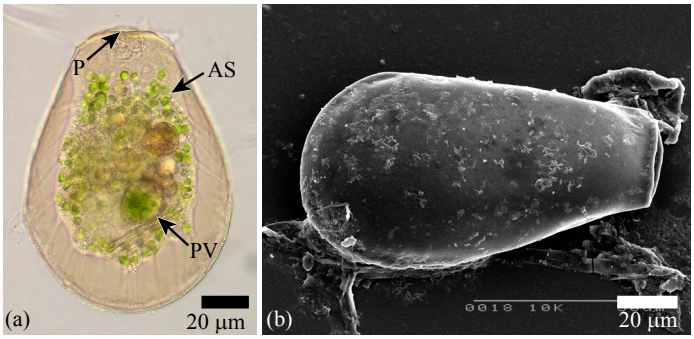

Fig. 1. Images of the testate amoebae *Hyalosphenia papilio*: (a) bright-field microscope image illustrating the amoeba itself and its content, P pseudostome (opening through which the amoeba pseudopods emerge), AS algal symbionts, PV phagocytic vacuoles; (b) SEM image illustrating the shell.

2. Experimental setup

Transmission off-axis DHM (Fig. 2) used for the present study is described in details in Refs. 19 and 20. It is based on a Mach-Zehnder configuration. Half-wave plates and neutral filters are used in conjunction with a polarizing beam splitter to control the light intensity in the two arms of the interferometer. The light source is a polarized laser diode emitting at 635 nm. Results presented here have been obtained with an Olympus 20X 0.4 NA microscope objective (MO). A field lens is inserted in the reference arm in order to obtain a coarse compensation of the phase curvature induced by the MO into the object wave, while the fine tuning compensation is numerically achieved during the hologram reconstruction process, as extensively described in Ref. 14. The camera is a 512 x 512 pixels, 8 bit, black and white CCD, with square pixels of 6.7 µm, and a maximal frame rate up to 25Hz. The field of view is 200 µm x 200 µm. The transverse resolution (around 1.5 µm) as well as the transverse scale calibration have been determined with a USAF 1951 resolution test target. All measurements have been achieved without any particular vibrations-insulating system: since a single hologram is required to reconstruct the complex diffracted wavefront, this is performed in a short time (down to 20 µs with our CCD), leading to high measurement stability. With a Pentium 4 2.8Ghz, the phase reconstruction rate, described in the next paragraph, is 15 frames/second.

#71852 - $15.00 USD Received 9 June 2006; revised 20 July 2006; accepted 24 July 2006

In the present work, the specimen is observed in a specifically designed chamber, principally composed by two microscope coverslips orthogonal to the optical axis. An aluminum frame maintains the two coverslips 4 mm distant, while fixations assure the watetightness of the chamber. One lateral side of the chamber is free to allow the introduction of a micropipette (MP) used to manipulate the specimen, or to change the perfusion medium during observation.[4] The manipulation method is similar to the so-called patch-clamp technique, in which thin MPs are used to maintain contact with a specific part of cells, for example the plasma membrane. These MPs are produced by the elongation of glass tubes during a controlled heating process. Their extremities, with a diameter around 1 micrometer, may then be polished to ensure a good contact with the cell membrane. Here, the specimen may be manipulated (translated or rotated) by one of these MPs, by using a little vacuum to maintain contact between the glass and the testate. To ensure good manipulation and rotation stability, the MP used during the final measurement had extremities about 10 μm, instead of the standard ones. The MP is fixed on a motorized rotating stage, and its position is adjusted with a micrometric xy-stage to place accurately its extremity on the rotation axis, minimizing therefore displacements of the specimen during rotation. A first micrometric xyz-stage allows moving the MP relatively to the chamber, to grab a specific specimen or to drag a selected specimen in a clean area of the preparation for observation, while a second xyz-stage allows moving simultaneously the MP and the chamber for a proper positioning in the field of view. Note that the chamber can be inclined relatively to the optical axis to allow picking up the desired specimen, in case it is laying on the bottom of the chamber due to gravity.

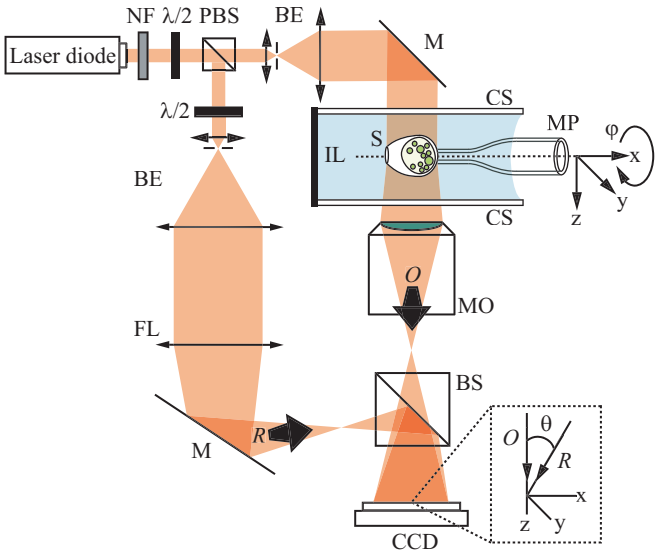

Fig. 2. Holographic microscope for transmission imaging: NF neutral density filter; PBS polarizing beam splitter; BE beam expander with spatial filter; λ/2 half-wave plate; MO microscope objective; FL field lens; M mirror; BS beam splitter; *O* object wave; *R* reference wave; MP micropipette; CS coverslip; S specimen; IL immersion liquid. Inset: a detail showing the off-axis geometry at the incidence on the CCD.

In a previous work,[12] the specimen were embedded in a MP with an internal diameter of 100 μm to allow their rotation in the system. Compared to this first approach, the patch-clamp technique used in this study presents two decisive improvements. Firstly, the MP is now out of the light path going through the specimen: in the previous setup, the MP was acting like a cylindrical lens, introducing astigmatism in the imaging system. Therefore, an index matching liquid was used to minimize this astigmatism, and a numerical procedure was additionally applied to compensate for the residual phase aberrations (see Refs. 20 and 21). Note that the

#71852 - $15.00 USD Received 9 June 2006; revised 20 July 2006; accepted 24 July 2006

index matching liquid used to compensate partially for the astigmatism needed to be carefully chosen and adapted to the used MP, what requested an additional calibration procedure, and also that the requested numerical procedure consisted potentially in an additional noise source when not conducted carefully. This first modification reduces drastically the complexity of the setup and increases therefore its ease of use. Secondly, the previous embedding technique was not applicable on living animal cells, because the perfusion of the cells within the MP was not possible. Furthermore, the current system is more versatile, allowing for facilitated specimen selection and manipulation, compared to the non-displaceable specimen embedded randomly in the MP.

Glycerol (n=1.473) is used here as immersion liquid, to minimize the number of the so-called 2π-jumps in the phase signal by minimizing the refractive index difference between the specimen and its surrounding medium, suppressing ambiguity during the unwrapping procedure involved in the reconstruction.[12] Note that the chamber is waterproof enough to also work with less viscous immersion media such as water or physiological solution.

3. Holograms processing and tomographic reconstruction

Digital holographic microscopy (DHM) provides quantitative measurement of the OPL distribution that enable to describe semi-transparent samples, such as living cells with a diffraction-limited transverse resolution and a sub-wavelength axial accuracy.[22] The hologram processing, to reconstruct the complex diffracted wavefront, is described in details in Refs. 19 and 20. Briefly, it consists in multiplying the hologram by a digital reference wave simulating an illumination wave, then a propagation calculation within the Fresnel approximation allows to reconstruct a focused image of the specimen in a plane of coordinates, where a digital phase correction is applied to compensate for the wave front curvature induced by the objective lens and other aberrations of the optical imaging system.

In DHM, the reconstructed phase distribution depends on both specimen thickness and specimen RI distribution.[22] If in first approximation the case of a weekly diffracting object is assumed, the optical path length of the collimated illuminating photons across the specimen is parallel to the optical axis. This assumption was found to be in very good agreement with the DHM data in the case of cellular imaging.[23] The reconstructed phase distribution is therefore directly proportional to this optical path length:

$$\varphi(x,y) = \int 2\pi/\lambda \, \Delta n(x,y,z)\, dz \,, \tag{1}$$

where z shows the optical axis direction, λ is the wavelength of the light source and $\Delta n(x, y, z)$ is the difference between the 3D specimen RI spatial distribution and the RI of the surrounding medium. Consequently, $\varphi(x,y)$ is only proportional to the projection of $\Delta n(x, y, z)$ along the z-axis.

To achieve the tomographic reconstruction, the specimen is rotated step by step in the system, covering a total angle of π. 180 equally spaced holograms were acquired at a rate of 0.5 Hz and individually reconstructed. The representation of the reconstructed phase data as a function of the angle is known as a sinogram. The 3D signal $\Delta n(x, y, z)$ can be reconstructed from the sinograms by a filtered backprojection algorithm (see for ex. Ref. 24). Instead of backpropagation[25] algorithm usually recommended in ODT, a backprojection is used consistently with the assumption of a phase proportional to the optical path length across the specimen. For this purpose, the standard inverse Radon transform was used and implemented slice-by-slice along the rotation axis. For further details about the validity of the employed tomographic technique, one should refer to Ref. 26, where it is shown that the so-called hybrid filtered backprojection equivalent to the reconstruction algorithm used in the present work, i.e. consisting in first a backpropagation in the Fresnel approximation of the measured wavefronts to the object plane followed by a backprojection algorithm, gives nearly equivalent results to the standard recommended backpropagation algorithm.

#71852 - $15.00 USD Received 9 June 2006; revised 20 July 2006; accepted 24 July 2006

4. Results and discussion

Tomographic reconstructions were performed on 5 different *Hyalosphenia papilio* during this study. Central cuts in the reconstructed 3D refractive index volumes for 4 different amoebae are presented on Fig. 3 and Fig. 4. On these images, the cellular body of the amoebae themselves insides their testate can be easily discriminated thanks to the large difference (>0.2) between the cell RI and the RI inside the testate.

One can note on these images that the refractive index inside the testate is lower compared to the surrounding medium. This is due to the fact that glycerol (n=1.473) was used as immersion liquid: the mix of some remaining water inside the testate with the surrounding glycerol explains this decrease of the refractive index value. Note that if the measurement was performed immediately after the immersion of the amoeba in the glycerol, the refractive index inside the test corresponded directly to water (n=1.33), while in the presented measurements, higher values are obtained, indicating clearly the presence of glycerol inside the test. The presence of glycerol around the cellular body may slightly change its volume, but no dramatic changes were noticed during cells preparation and observation.

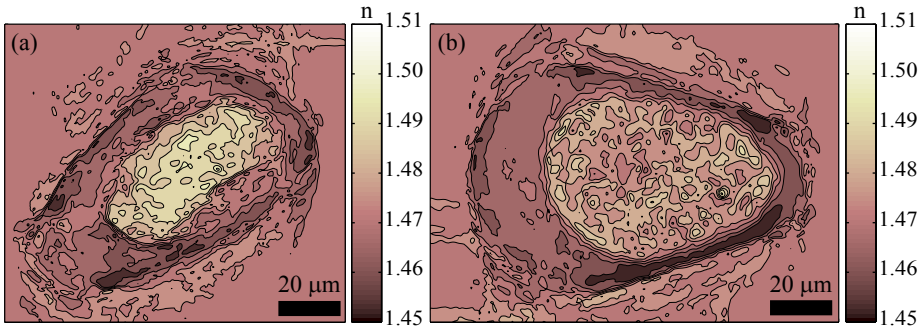

Fig. 3. Cuts in the tomographic reconstructions of 2 different *Hyalosphenia papilio*. Discrete values of the measured refractive index n are coded in false colors, the color-coding scales being displayed on the right part of each corresponding cut.

Morphometry measurements can be achieved on the tomographic reconstruction, to determine for example the biovolume of the amoebae. These volumes were evaluated by considering only the voxels with a refractive index value above an appropriate threshold. Note that the reconstructed volumes were first convoluted with a gaussian filter to minimize errors due to the reconstruction noise, and that the detected volumes distinct from the main cellular body were removed from counting.

The obtained results are presented in Table 1; the error ranges correspond to the optical resolution of the system. These volume measurements are compared in Table 1 with the estimation methods based on size measurements performed with light microscopy,[17-18] where such biovolumes estimations are calculated from the observed individuals using the formula for an ellipsoid:

$$V = \tfrac{4}{3}\pi \cdot w \cdot l \cdot d \cdot \tfrac{1}{8}, \qquad (2)$$

where *w*, *l* and *d* are respectively the width, the length and the depth of the amoeba, and 1/8 is a form factor.

The estimated errors on the volume estimation with Eq. (2) displayed in Table 1 correspond to an accuracy of 2 µm in the size measurements. DHM tomography clearly delivers the most precise estimations of the biovolumes, i.e. with the lowest standard error. This shows the advantage of taking into account the actual shape of the cellular body instead not an ellipsoid approximation, in which slightly errors in the dimension measurement lead to large variation in the volume estimation.

#71852 - $15.00 USD Received 9 June 2006; revised 20 July 2006; accepted 24 July 2006

Table 1. Estimated biovolumes for *Hyalosphenia papilio*.

Testate amoeba	Biovolumes [μm^3]	
	DHM tomography	Light microscopy
n°1: Fig. 3(a)	$6.54 \cdot 10^4 \pm 0.05 \cdot 10^4$	$2.8 \cdot 10^4 \pm 1.2 \cdot 10^4$
n°2: Fig. 3(b)	$7.36 \cdot 10^4 \pm 0.04 \cdot 10^4$	$3.7 \cdot 10^4 \pm 1.5 \cdot 10^4$
n°3: Fig. 4(a)	$6.54 \cdot 10^4 \pm 0.04 \cdot 10^4$	$4.9 \cdot 10^4 \pm 1.7 \cdot 10^4$
n°4: Fig. 4(b)	$8.09 \cdot 10^4 \pm 0.04 \cdot 10^4$	$3.2 \cdot 10^4 \pm 1.3 \cdot 10^4$
n°5: not presented	$3.94 \cdot 10^4 \pm 0.02 \cdot 10^4$	$2.5 \cdot 10^4 \pm 1.1 \cdot 10^4$
Means	$6.49 \cdot 10^4 \pm 0.04 \cdot 10^4$	$3.4 \cdot 10^4 \pm 1.3 \cdot 10^4$

The tomography also reveals that those volumes are under-estimated by nearly 50% with the actual standard method. This comparison illustrates the potential of DHM tomography for the precise and accurate estimation of biovolumes, which allows to determining biomasses. More generally, our results also show that in addition to the well-recognized problem of estimating the number of microorganisms in the environment,[27] more attention should be devoted to the estimation of the biovolume and biomass of individual species. A reliable estimate of biomass is crucial for understanding of the role of different microorganisms in the microbial food webs,[17,18,28] or the effect of environmental stress like organic pollutants or heavy metals on selected organisms in ecotoxicology.

At present, the whole reconstruction process involved in DHM tomography, including specimen manipulation, holograms acquisition/processing and tomographic reconstruction still requires too many operator interventions to calculate systematically the biovolumes of large amount of amoeba. However, as suggested above, this technique could help to derive allometric relationships that would greatly increase the precision of biovolumes and biomass estimates.

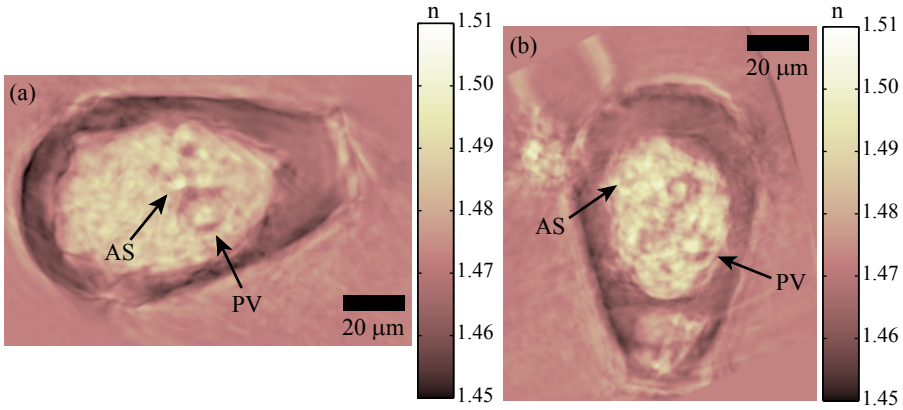

Fig. 4. Animations [1.3MB (a), 1.7MB (b)] through the tomographic reconstructions of two selected *Hyalosphenia papilio* presenting some clearly visible inner structures tentatively identified as algal symbionts (AS) and phagocytic vacuoles (PV). The gray-level scales of the measured refractive index n are displayed on the right part of each corresponding cut.

The actual resolution in the tomographic reconstruction is mainly limited because of mechanical instabilities. Theoretically, the optical resolution in all three dimensions for the tomographic reconstructions is about 1.5 µm, but an inaccurate centering of the MP on its rotation axis leads to a precession movement of the specimen during rotation that tends to derogate from the final tomography resolution. Therefore, during the reconstruction, a re-centering numerical procedure based on the MP edges detection in the phase images has been applied. Even if it is not currently possible to identify accurately all the symbiotic algae, with

#71852 - $15.00 USD Received 9 June 2006; revised 20 July 2006; accepted 24 July 2006

diameter around 3 μm,[29] and other organelles present in the amoeba cellular body, some of these organelles (principally the phagocytic vacuoles, but also some algal symbionts) are visible in the tomographic reconstructed volumes. Due to discrete color scale, it may be difficult to notice them in Fig. 3, but the continuous color scale make their spherical shape clearly visible, as shown in Fig. 4, especially in the linked movies presenting animations through the reconstructed volumes, in which they appear like spheres in the cellular body. This shows that potentially, the tomographic reconstructions could also be used to solve the problem of symbiotic algae counting and volume estimate inside the amoeba cellular body.

5. Conclusion

The present work illustrates that DHM tomography, with a resolution better than 3 μm, may successfully be applied to living specimen tomography. In comparison to a previous paper,[12] the presented technique, using a patch clamp micropipette to manipulate and rotate the specimen in a dedicated observation chamber, is much more flexible and opens wide perspectives in 3D cell imaging: the 3D quantitative refractive index distributions furnish invaluable data on the cell components optical properties, potentially leading to information about organelles intracellular distribution. Furthermore, it has been shown that morphometric measurements may be extracted from the tomographic data, by detecting for example the extension of the cellular body thanks to its specific refractive index contrast within the 3D reconstructions. The presented results shed new light on the biovolume estimation technique of testate amoeba, by stressing that the common biovolume measurement technique under-estimates systematically the actual values by 50%.

Acknowledgements

This work has been supported by the Swiss National Science Foundation (grant n° 205320-103885/1) and by EU project RECIPE (Reconciling Commercial Exploitation of Peat With Biodiversity in Peatlands Ecosystems). RECIPE is partly supported by the European Commission (n° EVK2-2002-00269) and partly, for the Swiss partners EPFL and WSL-AR, by the Swiss Federal Office for Education and Science (SER n° 01.0438-1).

The SEM image of Fig. 1(b) was kindly provided by Dr. Jerry Kudenov and Keiko Kishaba, University of Alaska, Anchorage.

The authors also would like to thank the people at Lyncée Tec SA (www.lynceetec.com), PSE-A, CH-1015 Lausanne, for their enthusiasm and their constructive comments during the paper preparation.